



**HAL**  
open science

## Study of the influence of the supersaturation coefficient on scaling rate using the pre-calcified surface of a quartz crystal microbalance

Hélène Cheap-Charpentier, Olivier Horner, Jean Lédion, Hubert Perrot

### ► To cite this version:

Hélène Cheap-Charpentier, Olivier Horner, Jean Lédion, Hubert Perrot. Study of the influence of the supersaturation coefficient on scaling rate using the pre-calcified surface of a quartz crystal microbalance. *Water Research*, 2018, 142, pp.347 - 353. 10.1016/j.watres.2018.05.052 . hal-01836183

**HAL Id: hal-01836183**

**<https://hal.sorbonne-universite.fr/hal-01836183>**

Submitted on 17 Dec 2018

**HAL** is a multi-disciplinary open access archive for the deposit and dissemination of scientific research documents, whether they are published or not. The documents may come from teaching and research institutions in France or abroad, or from public or private research centers.

L'archive ouverte pluridisciplinaire **HAL**, est destinée au dépôt et à la diffusion de documents scientifiques de niveau recherche, publiés ou non, émanant des établissements d'enseignement et de recherche français ou étrangers, des laboratoires publics ou privés.

1  
2  
3  
4  
5  
6  
7  
8  
9  
10  
11  
12  
13  
14  
15  
16  
17  
18  
19  
20  
21  
22  
23  
24  
25

## **Study of the influence of the supersaturation coefficient on scaling rate using the pre-calcified surface of a quartz crystal microbalance**

Hélène Cheap-Charpentier <sup>a,b\*</sup>, Olivier Horner <sup>a,b</sup>, Jean Lédion <sup>a,c</sup>, and Hubert Perrot <sup>b</sup>

<sup>a</sup> EPF – Graduate School of Engineering, 3 bis rue Lakanal, 92330 Sceaux, France.

<sup>b</sup> Sorbonne Universités, UPMC Université Paris 06, CNRS, Laboratoire Interfaces et Systèmes Electrochimiques, 4 place Jussieu, F-75005, Paris, France.

<sup>c</sup> AMVALOR, 151 Boulevard de l'Hôpital, 75013 Paris, France.

\* Corresponding author: Tel.: +33 1 41 13 42 85

*E-mail address:* [helene.cheap-charpentier@epf.fr](mailto:helene.cheap-charpentier@epf.fr) (H. Cheap-Charpentier)

### **Abstract**

Scale deposition is a common issue in industrial plants, which creates technical problems, *i.e.* reduction of heat transfer, decrease of flow rate due to an obstruction of pipes. Therefore, the development of some appropriate methods based on well suitable *in situ* sensors to evaluate and predict the scaling propensity of water is a major concern in current research. This would be a good strategy for the optimization of anti-scaling treatments.

In this study, scaling tests were carried out using a sensitive sensor, which has been developed using a quartz crystal microbalance with a pre-calcified electrode surface (SQCM). This technique allowed studying the influence of the supersaturation on the scaling rate. The set-up was tested with different water samples which were brought to a given supersaturation coefficient by degassing the dissolved CO<sub>2</sub>. The prediction of the scaling propensity of water

1 was then possible through the relationship between the scaling rate on a pre-calcified surface  
2 and the supersaturation coefficient. In addition, the kinetics of CaCO<sub>3</sub> deposit on the pre-  
3 calcified SQCM surface was found to be slower for natural water than for synthetic water  
4 (same calcium concentration). Furthermore, the activation energy for scale deposit, in  
5 synthetic water, was found to be 22 kJ.mol<sup>-1</sup>, which may be related to the diffusion of ions  
6 and/or CaCO<sub>3</sub> nuclei in solution.

7

8 *Keywords:* calcium carbonate; scaling propensity; quartz crystal microbalance; pre-calcified  
9 surface.

10

11 *Abbreviations:*

12 QCM: Quartz Crystal Microbalance with a regular bare electrode surface;

13 SQCM: Quartz Crystal Microbalance with a pre-calcified electrode surface;

14 TOC: Total Organic Carbon;

15 XRD: X-Ray Diffraction

16

## 17 **1. Introduction**

18 Scale deposit on solid surfaces causes serious problems in many industries using or  
19 processing water, e.g. in cooling systems (Abd-El-Khaled and Abd-El-Nabey, 2013) or in  
20 heat exchangers (Yang, 2002). Indeed, the thickness of the scale deposit may limit thermal  
21 exchanges or the water flow in pipes. The use of chemicals is a common approach to control  
22 scale deposit. However, those chemicals may have an important impact on environment, *i.e.*  
23 in the eutrophication process. On the one hand, scale deposit could occur when water  
24 becomes supersaturated, *i.e.* the product of ions activities,  $[Ca^{2+}] \times [CO_3^{2-}]$ , exceeds the  
25 solubility product  $K_{sp}$  of CaCO<sub>3</sub> (Xyla, et al., 1991). On the other hand, scale deposit may

1 take place due to an external cause, *i.e.* the introduction of a substrate or seed crystals (Donnet  
2 et al., 2010). Thus, preventing scale formation has raised a great interest. It is relevant to  
3 develop some efficient methods based on *in situ* sensors to follow the scaling propensity of  
4 water in order to prevent scale deposit.

5 Some methods based on the determination of the scaling rates have been developed in  
6 order to estimate the scaling propensity of water (Hui and Lédion, 2002; Leroy et al., 1993;  
7 Al Nasser and Al Salhi, 2013). For example, Hui et al. (Hui et al., 2003) have studied the  
8 scaling rates using witness tubes with pre-calcified surface. Zhang et al. (Zhang et al., 2001)  
9 considered thermodynamic models in order to evaluate the tendency for scaling from  
10 solutions and kinetics models to predict the rate of scaling. The use of chronoamperometry at  
11 constant reduction potential was the more fruitful approach to investigate the scaling rate  
12 (Gabielli et al., 1996; Lédion et al., 1985). However, correlation between supersaturation  
13 coefficient and scaling rate on a solid surface was not very well developed in literature. Some  
14 discrepancies were detected between real deposit on solid surfaces and scaling rates estimated  
15 from predictive models based on thermodynamic data where precipitation tendency were  
16 predicted (Hasson et al., 1996).

17 Recently, a quartz crystal microbalance with a pre-calcified sensitive surface (SQCM)  
18 has been developed (Chao et al., 2014a). The sensitive surface could be used as an adsorption  
19 layer for CaCO<sub>3</sub> nuclei present in water. It was installed in a cell simulating an industrial fluid  
20 stream with a laminar flow. A preliminary relationship was obtained between the  
21 instantaneous scaling rate and the supersaturation coefficient of synthetic water at different  
22 concentrations of Ca<sup>2+</sup> ([Ca<sup>2+</sup>] in the range 60 mg.L<sup>-1</sup> - 200 mg.L<sup>-1</sup>) and at a given temperature  
23 (T=35°C). This opens the possibility to quantify the scaling propensity of a tested water.

24 In this work, the pre-calcified QCM electrode was installed in a miniaturized lab-made  
25 cell. This original set-up was tested with synthetic water which was brought to a given

1 supersaturation coefficient related to the precipitation of calcium carbonate by CO<sub>2</sub> degassing  
2 (Gauthier et al., 2012; Chao, 2014b). Indeed, only calcium carbonate (CaCO<sub>3</sub>), one of the  
3 most abundant mineral scale compound (Keysar, 1994), will be considered in this study. This  
4 work is focused on calcium carbonate scaling, *i.e.* the deposit of calcium carbonate on a  
5 surface, and not with calcium carbonate precipitation in solution, *i.e.* the appearance of a Ca  
6 CO<sub>3</sub> solid phase within the bulk solution. The deposit kinetics of calcium carbonate nuclei on  
7 the active electrode of the SQCM was measured at different supersaturation coefficients for  
8 two temperatures (T=30°C and 40°C), either for a synthetic or a natural water. Indeed, it was  
9 possible to compare, in a very sensitive way, the scaling propensity of a synthetic and a  
10 natural mineral water (same calcium concentration). Thus, this work investigates, thanks to  
11 the pre-calcified QCM electrode, the effect of several parameters like supersaturation level,  
12 temperature and composition of water on scaling rate. For the first time, the activation energy  
13 of the scaling process on the pre-calcified surface, for synthetic water, was investigated.

14

## 15 **2. Materials and methods**

### 16 *2.1. Reactants*

17 Synthetic waters were pure solutions, which only contained Ca<sup>2+</sup> and CO<sub>3</sub><sup>2-</sup> ions. The  
18 synthetic waters (100 or 200 mg/L in calcium, depending on the experiment) used in this  
19 work were prepared by dissolving solid calcium carbonate (AnalaR NORMAPUR VWR,  
20 99.7% purity) in pure water (Milli.Q water, 18.2 MΩ cm resistivity and TOC <5 mg L<sup>-1</sup>) by  
21 bubbling CO<sub>2</sub> gas. After the solid dissolution, the pH of the solution was about 5.2-5.5. Under  
22 those experimental conditions, no spontaneous precipitation of CaCO<sub>3</sub> occurred. The solution  
23 was then filtered with a Millipore filter (514-8073 Whatman, 0.45 μm porosity) to remove  
24 any impurities. Salvetat® water is a commercial natural water, which contains the following

1 elements (Table 1). The ions and TOC concentrations in Salvetat water have been determined  
 2 according to IANESCO laboratory (Poitiers, France) titration report.

3

4 **Table 1:** Concentration of ions in Salvetat® water.

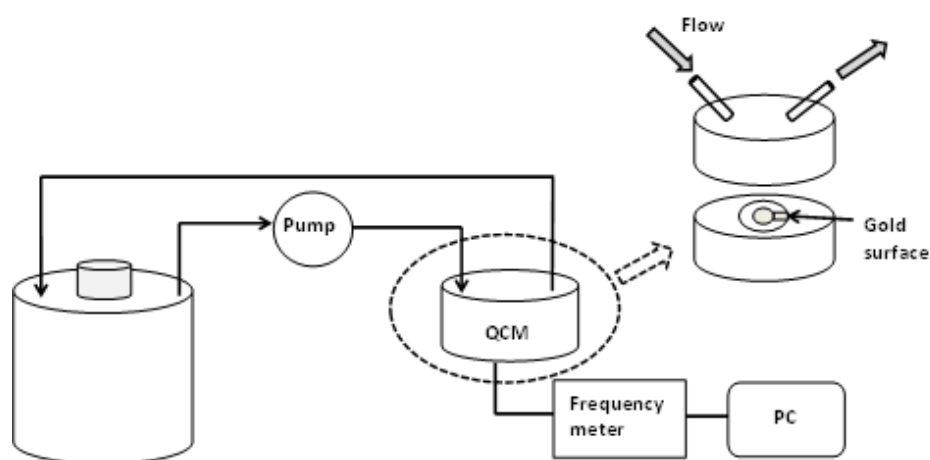
Ions	Ca <sup>2+</sup>	Mg <sup>2+</sup>	HCO <sub>3</sub> <sup>-</sup>	Cl <sup>-</sup>	SO <sub>4</sub> <sup>2-</sup>	Na <sup>+</sup>	K <sup>+</sup>	TOC
Concentration (mg.L <sup>-1</sup> )	180	8.7	634	4.6	31	5.7	1.7	0.4

5

6 *2.2. QCM set-up*

7 A quartz crystal microbalance with a pre-calcified electrode surface (SQCM) was used  
 8 to measure the mass of calcium carbonate deposited on the pre-calcified surface (Figure 1).

9



10

11

12 **Figure 1:** Scheme of a SQCM set up.

13

14 The volume of the SQCM cell was 500 μL. The flow rate was set to 2 mL.min<sup>-1</sup> using  
 15 a peristaltic pump. The water jet arrived at 45° on the flat surface of the modified electrode.

1 The bare surface of the electrode consisted in a 5 mm diameter gold disc covering a 9 MHz  
2 AT cut quartz crystal resonator (AWS, Spain).

3 The pre-calcifying process was performed in a classical “three-electrode” set-up with  
4 the bare gold electrode acting as a working electrode. All the electrodes were inserted in a  
5 submerged impinging jet cell (flow rate of 300 mL.min<sup>-1</sup>), with a synthetic water (200 mg.L<sup>-1</sup>  
6 Ca<sup>2+</sup>) at 30°C.

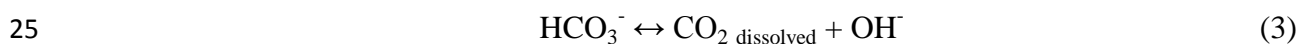
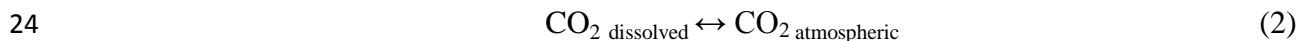
7 The frequency of the microbalance device was measured by a frequency-counter (Fluke  
8 PM6685). The mass deposited onto the bare or the pre-calcified surface of the sensor was  
9 measured over time from the microbalance frequency change (Bizet et al., 2000; Chao et al.,  
10 2014a). The frequency change  $\Delta f$  of the quartz resonator due to the deposition of the scale on  
11 the working electrode was proportional to the mass change  $\Delta m$  according to Sauerbrey  
12 equation (Sauerbrey et al., 1959):

$$\Delta f = -K_s \cdot \Delta m \quad (1)$$

13  
14  
15  
16 where  $K_s$  is the sensitivity factor ( $K_s$ )<sup>-1</sup> = 1,09 ng per Hz for an electrode area of 0.2 cm<sup>2</sup>.

### 18 2.3. Preparation of water with a given supersaturation coefficient $\delta$

19 Stable solutions of calcium carbonate were brought to a given supersaturation  
20 coefficient ( $\delta$  coefficient) by CO<sub>2</sub> degassing (Lédion et al., 1997; Gauthier et al., 2012; Chao  
21 et al., 2014b). Indeed, the degassing of dissolved CO<sub>2</sub> is accelerated by stirring the water  
22 sample. As the CO<sub>2</sub> degasses, the concentration of [H<sup>+</sup>] decreases, so the concentration of  
23 [OH<sup>-</sup>] or the pH increases according to the following equations:



1 As a consequence, the saturation level of the solution increases with stirring.  
2 Supersaturation coefficient  $\delta$ , the extent of deviation of the solution from the equilibrium  
3 condition, is the driving force for the formation of a  $\text{CaCO}_3$  crystalline phase in aqueous  
4 solutions.  $\delta$  is defined according to the following equation (5): (Legrand et al., 1981)

$$5 \quad \delta = [\text{Ca}^{2+}] \times [\text{CO}_3^{2-}] / K'_{\text{sp}} \quad (5)$$

6 where  $[\text{Ca}^{2+}]$  and  $[\text{CO}_3^{2-}]$  are the concentrations of calcium ions and carbonate ions  
7 respectively, and  $K'_{\text{sp}}$  is the apparent solubility product of calcium carbonate. As stated above,  
8 the supersaturation level  $\delta$  of the studied water was increased by using a moderate stirring  
9 (400 rpm) of the solution. For each test, the synthetic water was initially brought to the same  
10 supersaturation coefficient ( $\delta=40$ ), below the homogeneous precipitation threshold. The pH of  
11 the solution was measured as a function of time using a pH-meter (Radiometer pHM220). The  
12 pH electrode was purchased from Radiometer Analytical, and the saturated calomel electrode  
13 (Radiometer Analytical) was used as a reference electrode. When the solution reached a given  
14  $\delta$  value (i.e. a given pH value), the stirring was stopped and all the openings of the beaker  
15 were hermetically sealed. The value of  $\delta$  was maintained below the spontaneous precipitation  
16 threshold.

17

#### 18 *2.4. X-ray diffraction (XRD)*

19 The XRD method was used in order to determine crystalline polymorphs of  $\text{CaCO}_3$   
20 formed on the gold surface. XRD measurements were performed at room temperature with  
21  $\text{Cu-K}\alpha$  radiation (1.52 Å) using a Panalytical (Empyrean Diffractometer Panalytical) device  
22 with prefix configuration. Crystalline forms of the  $\text{CaCO}_3$  layer forming the pre-calcified  
23 surface were determined from spectra obtained by XRD measurements.

24

#### 25 *2.5 Scaling rate equation*



1  
2  
3  
4  
5  
6  
7  
8  
9  
10  
11  
12  
13  
14  
15  
16  
17  
18  
19  
20

During this scaling process, the balance between precipitation and dissolution of scaling can be described by the following equation:



where R represents  $Ca^{2+}$  and  $CO_3^{2-}$  species and P represents calcium carbonate in solid phase.  $k_+$  and  $k_-$  are the rate constants related to the reactions of precipitation or dissolution, respectively. The relationship between the reaction rate,  $V_S$ , and the free energy,  $\Delta G$  is given by equation (7): (Blum et al., 1990)

$$V_S = \frac{d[CaCO_3]}{dt} = -\frac{S}{V} k \left[ 1 - \exp\left(\frac{\Delta G_{pre} + \Delta G_{dis}}{R_g T}\right) \right]^n = -\frac{S}{V} k \left[ 1 - \exp\left(\frac{\Delta G}{R_g T}\right) \right]^n \tag{7}$$

where  $V_S$  is the reaction rate, S is the reaction surface, V is the volume of the solution,  $\Delta G_{pre}$  and  $\Delta G_{dis}$  are, respectively, the free energy released in  $CaCO_3$  formation process and the free energy expended in dissolution of calcium carbonate,  $\Delta G$  is the total free energy of the reaction, k is the rate constant of the reaction and n the reaction order.  $\Delta G$  depends on the supersaturation level,  $\delta$ , of the solution according to the following equation:

$$\Delta G = \frac{R_g T}{2} \ln \delta \tag{8}$$

For the scaling rate ( $\delta > 1$ ), equation 7 can be rewritten as:

$$\log V_S = \log k' + n \times \log [\delta^{1/2} - 1] \tag{9}$$

1 where  $V_s$  ( $\mu\text{g}\cdot\text{cm}^{-2}\cdot\text{min}^{-1}$ ) is the scaling rate,  $k'$  is the rate constant for deposit ( $k' = (S/V) k$ )  
2 and  $n$  is the apparent reaction order (Morse et al., 2007).

3

### 4 **3. Results and discussion**

5

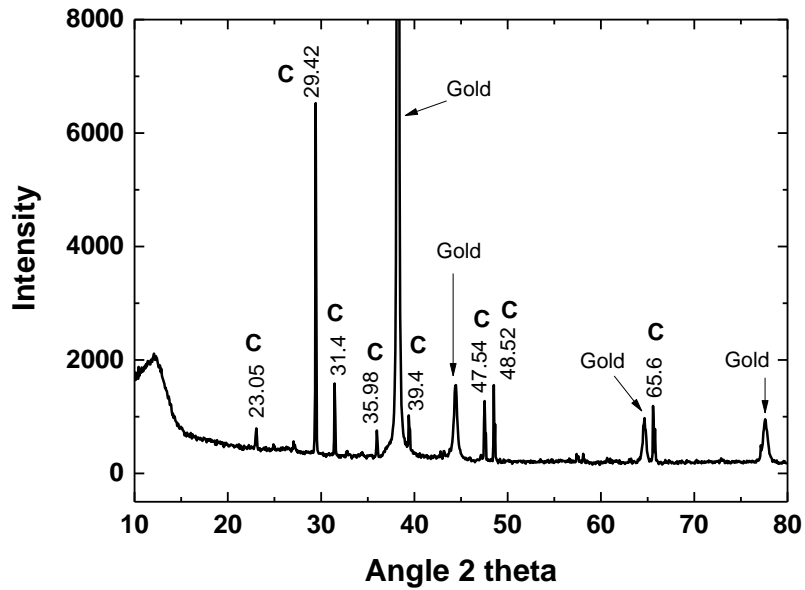
#### 6 *3.1. Pre-calcification of the sensitive surface of QCM*

7

8 The sensitive surface of QCM can be initially covered by a calcium carbonate layer to  
9 obtain the SQCM sensor (Gabrielli et al., 1998; Peronno et al., 2015). The potential applied to  
10 the working electrode was  $-1$  V/SCE, leading to the reduction of the dissolved dioxygen to  
11 produce hydroxyl ions. The formed hydroxyl ions increased the local pH near the electrode  
12 surface (Tlili et al., 2003) which led to the transformation of bicarbonate ions into carbonate  
13 ions. The carbonate ions reacted with calcium ions to form a  $\text{CaCO}_3$  precipitate on the surface  
14 of the working electrode.

15 The pre-calcifying experiment was stopped when the current, recorded during calcium  
16 carbonate deposition, reached a low residual constant value of a few micro amps. This  
17 indicates that the electrode surface was fully recovered by the  $\text{CaCO}_3$  film. In these  
18 experimental conditions, the solid phase formed on the electrode surface was pure calcite, the  
19 most thermodynamics form of calcium carbonate (Morse et al., 2007), as shown in Figure 2:

20



1

2 **Figure 2:** XRD spectrum of the CaCO<sub>3</sub> layer formed during the pre-calcifying process.

3 C: calcite.

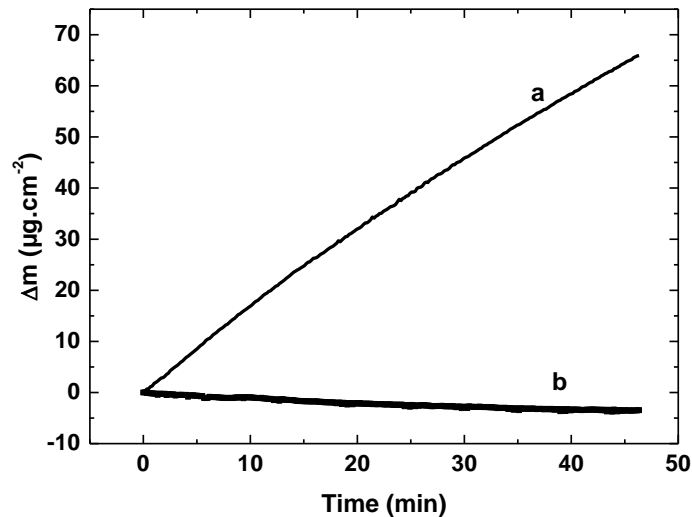
4

5 Obtaining pure calcite is likely to be due to a moderate kinetics of deposition. If the  
 6 kinetics of deposition would increase, a mixture of calcite and aragonite would be observed.  
 7 This process of layer formation is highly reproducible and the CaCO<sub>3</sub> layer was stable over  
 8 time (Gabielli et al., 1999).

9

10 *3.2. Comparison of the bare surface and the pre-calcified surface (pure calcite) of the sensor*  
 11 *towards scaling*

12 Figure 3 shows the curves of mass change as a function of time for synthetic water  
 13 ([Ca<sup>2+</sup>]=200 mg/L, T=30°C) for a pre-calcified surface (pure calcite), and a bare gold surface  
 14 as the sensitive part of the sensor.



1

2 **Figure 3:** Mass change as a function of time for synthetic water with (a) a pre-calcified  
 3 surface (pure calcite) (scaling time  $V_s=1.2 \mu\text{g}\cdot\text{cm}^{-2}\cdot\text{min}^{-1}$ ) and (b) a bare gold surface (initial  
 4  $[\text{Ca}^{2+}]=200 \text{ mg/L}$ ,  $T=30^\circ\text{C}$ , flow rate= $2 \text{ mL}\cdot\text{min}^{-1}$ ,  $\delta=40$ ).

5

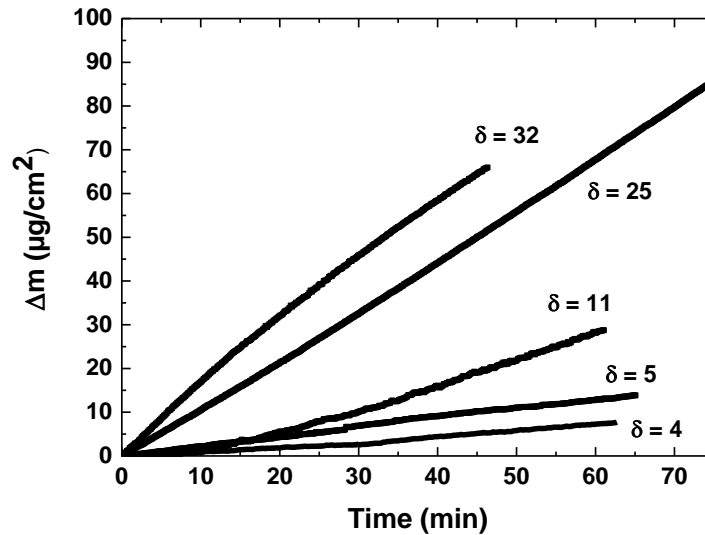
6 In Figure 3b, the mass change detected on the bare gold surface was roughly constant.  
 7 This indicates that no  $\text{CaCO}_3$  deposition was detected by the QCM sensor with no pre-  
 8 calcified surface. On the contrary,  $\text{CaCO}_3$  deposit is immediately observed on the pre-  
 9 calcified surface of the sensor (Figure 3a). It should be noticed that the mass deposited on the  
 10 pre-calcified surface increased linearly over time.

11 In this work, the pre-calcified surface of the sensor is very sensitive towards  $\text{CaCO}_3$   
 12 nuclei adsorption, compared to a bare gold surface. This result validated the use of a pre-  
 13 calcified surface for scaling tests. This is in line with the results obtained from the literature.  
 14 (Hui et al., 2003) on titanium or copper tubes. Indeed, they showed that the scaling rate was  
 15 enhanced when the inner surface of the tubes was pre-calcified.

16

17 *3.3. Supersaturation level vs scaling rate for synthetic water*

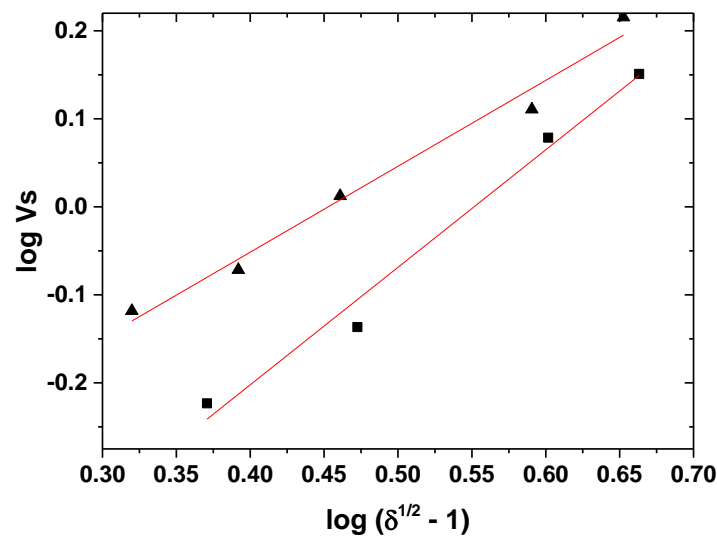
1 Kinetics of calcium carbonate nuclei deposit on a pre-calcified surface was determined  
2 by the SQCM device for synthetic water with given  $\delta$  coefficients (see Materials and  
3 methods). Figure 4 shows the influence of the supersaturation level over the mass change on a  
4 pre-calcified surface (pure calcite) as a function of time.



5  
6 **Figure 4:** Mass change as a function of time: influence of the supersaturation coefficient  
7 ( $T=30^\circ\text{C}$ , flow rate= $2\text{ mL}\cdot\text{min}^{-1}$ , pre-calcified surface of the sensor made of pure calcite).

8  
9 Figure 3 shows that the mass change on the pre-calcified surface (pure calcite)  
10 depends strongly on the supersaturation level of the studied solution (with the others  
11 parameters constant). The higher was the degree of supersaturation, the faster were the scaling  
12 rate and the amounts of deposit. This suggests that the number of  $\text{CaCO}_3$  nuclei strongly  
13 affects the scaling rates (Chao et al., 2014a). Moreover, SQCM could detect  $\text{CaCO}_3$  nuclei,  
14 even at very low supersaturation coefficient ( $\delta=4$ ). Recently, Chao et al. showed, by using  
15 Small Angle X-rays Scattering (SAXS) spectroscopy, that  $\text{CaCO}_3$  nuclei were present in  
16 synthetic water before the homogeneous precipitation (Chao et al., 2014b). These  $\text{CaCO}_3$   
17 nuclei can be detected also in the early stage of the experiments with this measurement  
18 (Demichelis et al., 2011).

1 It should be noticed that the scaling rate  $V_s$ , on a pre-calcified surface, was constant over time  
 2 for given experimental conditions. For each  $\delta$  value, the scaling rate  $V_s$  can be calculated from  
 3 the slope of the linear regression related to the mass change vs time curve (Fig. 3).  $V_s$   
 4 characterizes the scaling propensity of water (Chao et al., 2014a). A plot of the logarithm of  
 5 scaling rate as a function of the logarithm of the supersaturation coefficient could be linearly  
 6 fitted using equation 9, as detailed in the Materials and Methods part (Figure 5).



8  
 9 **Figure 5:** Logarithm of the scaling rate  $V_s$  as a function of the logarithm of  $\delta$  at (■) 30°C and  
 10 (▲) 40°C (flow rate=2 mL.min<sup>-1</sup>, pre-calcified surface of the sensor made of pure calcite).

11  
 12 The data related to the linear fit are summarized in Table 2.

13 **Table 2:** Summary of data obtained from fitted curves (see text for signification of the  
 14 parameters).

T (°C)	k/SI	n	R <sup>2*</sup>
30	0.19	1.3	0.95
40	0.36	1	0.98

15 \* Goodness-of-fit measure for the linear regression model.

1 As shown in Figure 4, the scaling rates of calcium carbonate were found to depend  
2 strongly on the value of the supersaturation level of the studied solution, for a given water  
3 (Zhang et al., 2001; Chen et al., 2005; Parlaktuna and Okandan, 1989; Abdel-Aal et al., 2002;  
4 Ben Amor et al., 2004). The scaling rate increased with  $\delta$ , in agreement with the results from  
5 literature. For example, Al Nasser et al. (Al Nasser et al., 2013) showed that the deposit rate  
6 on steel plates immersed in a scale forming solution increased when  $\delta$  increased. Koutsoukos  
7 and Kontoyannis (Koutsoukos and Kontoyannis, 1984) measured the scaling rate of calcium  
8 carbonate precipitation from aqueous solution by following the disappearance of calcium ion  
9 over time. They showed that the scaling rate increased with the supersaturation coefficient.

10 It must be noted that the orders of reaction  $n$  shown in Table 2 are of the same order of  
11 magnitude as those reported in literature. Indeed, an apparent order of 1.3 ( $T = 22^\circ\text{C}$ ) was  
12 reported for the  $\text{CaCO}_3$  growth on nuclei (Packter, 1968). Moreover, Kitano and Hood  
13 (Kitano and Hood, 1965) found a reaction order of *ca* 1 for the growth of  $\text{CaCO}_3$ . Parsiegl  
14 and Katz (Parsiegl and Katz, 1999) have reported an apparent order of 1 for calcite growth at  
15 low pH and low carbonate concentration. However, in their experiment they have investigated  
16 the kinetics of calcite growth. In this work, the  $\text{CaCO}_3$  layer was immobilized on a gold  
17 surface, and the scaling rate is related to the adsorption of nuclei formed in solution, likely as  
18 in a real scaling phenomena. In “natural conditions”, scaling phenomena occur on a surface  
19 for moderate supersaturation levels.

20

### 21 *3.4. Influence of the temperature on scaling rate in synthetic water*

22 SQCM was performed at higher temperature. The choice of the higher but moderate  
23 temperature ( $40^\circ\text{C}$ ) prevent the risk of precipitation of water at the beginning of the  
24 experiment. Figure 4 shows that the scaling rates established at  $40^\circ\text{C}$  were higher than those  
25 obtained at  $30^\circ\text{C}$ . This result is in agreement with previous studies (Al Nasser and Al Salhi,

1 2013; Ben Amor et al., 2004). Indeed, the solubility of  $\text{CaCO}_3$  decreases when the  
2 temperature increases (Plummer and Busenberg, 1982) and the temperature dependence on  
3 the scaling rate may affect the growing process on the pre-calcified surface (Hillig, 1966).  
4 According to the Arrhenius law, the calculated activation energy (from temperatures  $T=30^\circ\text{C}$   
5 and  $40^\circ\text{C}$ ) in the experimental conditions of this work was found to be  $22 \text{ kJ}\cdot\text{mol}^{-1}$ .

6 In literature, values of activation energies have been reported for surface controlled  
7 processes involving  $\text{CaCO}_3$  precipitation on crystal seeds. For example, Koutsoukos and  
8 Kontoyannis (Koutsoukos and Kontoyannis, 1984) found an apparent activation energy of  
9  $155 \text{ kJ}\cdot\text{mol}^{-1}$  for a growth process on  $\text{CaCO}_3$  seeds, suggesting that the calcium carbonate  
10 precipitation was surface-controlled in aqueous solution. An activation energy of  $46 \text{ kJ}\cdot\text{mol}^{-1}$   
11 was also reported for crystal growth on seed crystals of calcite (Nancollas and Reddy, 1971;  
12 Cassford and al., 1983; Xyla et al., 1991). In the present work, it must be noticed that the  
13 activation energy ( $22 \text{ kJ}\cdot\text{mol}^{-1}$ ) is related to a scaling process on an immobilized  $\text{CaCO}_3$  layer.

14 The influence of the flow rate on scale deposition was further investigated, in order to  
15 see if the activation energy determined in this study is related to diffusion (Fig. S2 in  
16 Supplementary Information). It was shown, by using the SQCM set-up with synthetic water  
17 ( $T=30^\circ\text{C}$ ,  $\delta=20$ , pre-calcified surface of the sensor made of pure calcite) that the kinetics of  
18 scale deposition increased with the flow rate. This suggests that the kinetics of scale  
19 deposition may be controlled by the diffusion of ions and/or  $\text{CaCO}_3$  nuclei in solution. In a  
20 previous work, the activation energy related to the dissolution process of vaterite was found to  
21 be  $24 \text{ kJ}\cdot\text{mol}^{-1}$  and was typical of the ion diffusion in aqueous solution (Brecevic and Kralj,  
22 2007).

23

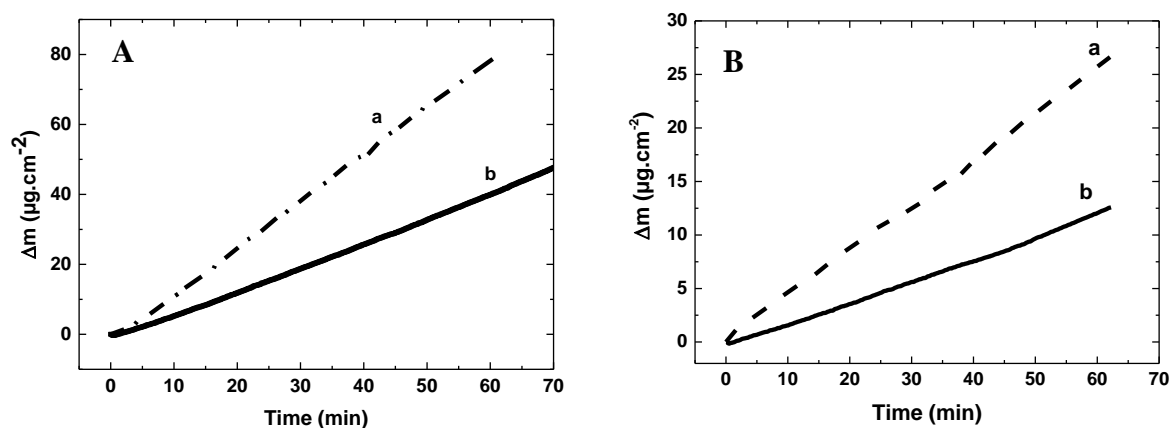
24 *3.5. Natural water vs synthetic water*



1 The Salvetat water is a natural water, which is very close to synthetic water, *i.e.* a  
 2 comparable amount of bicarbonate and calcium, and a very low content in other ions,  
 3 especially  $Mg^{2+}$  and  $Cl^-$  ions. The FT-IR spectrum of the precipitate obtained from the  
 4 Salvetat water is very similar to that of the pure calcium carbonate used for synthetic water  
 5 (Fig. S1 in Supplementary Information). In addition, there are no silicates or phosphates  
 6 species detectable in Salvetat water precipitate. As the Salvetat water is naturally aggressive,  
 7 the presence of  $CaCO_3$  germs at the beginning of the SQCM experiment is avoided. Thus, the  
 8 Salvetat water can be used to show the influence on scaling rate of elements that are not well  
 9 characterized but potentially present in water, *i.e.* natural organic substances and/or suspended  
 10 matter.

11 The mass change of the scale quantity deposited on the pre-calcified surface from a  
 12 synthetic water ( $[Ca^{2+}]=200\text{ mg.L}^{-1}$ ) and from a natural water (Salvetat,  $[Ca^{2+}]=180\text{ mg.L}^{-1}$ )  
 13 were investigated by using the SQCM set-up (Figure 6):

14



15 **Figure 6:** (A) Mass change of scale deposited from (a) synthetic water ( $[Ca^{2+}]=200\text{ mg.L}^{-1}$ ,  
 16  $\delta=20$ ), (b) Salvetat water ( $\delta = 21$ ). (B) Mass change of scale deposited from (a) Salvetat water  
 17 ( $\delta = 8.45$ ) and (b) Salvetat water diluted at 50% ( $\delta = 9.60$ ). Flow rate= $2\text{ mL.min}^{-1}$ ,  $30^\circ\text{C}$ , pre-  
 18 calcified surface of the sensor made of pure calcite.

19

1           Figure 6A shows that the SQCM is sensitive enough to determine the mass change in  
2 natural water. The results showed that the scaling rate is lower for the natural water (curve b)  
3 than for the synthetic water (curve a). A previous study using electrochemical QCM (EQCM)  
4 has shown that organic molecules with carboxylic groups were very efficient to inhibit  
5 towards calcium carbonate scaling (Peronno et al., 2015). The effect of humic substances  
6 (Chao et al., 2014a) and kaolinite (Chao, 2016) were investigated by using SQCM. It was  
7 shown that the average scaling rate decreased when the humic substance concentration  
8 increased. SQCM also showed that kaolinite had little influence on the scaling propensity of  
9 water. A slowdown of nucleation kinetics was also observed in the presence of clay  
10 suspensions (Hui et al., 2004).

11           As previously discussed the Salvetat water is, very close to synthetic water but also  
12 contains some elements that are not well characterized as organic substances (TOC of 0.4  
13 mg/L) or inorganic substances. The data shown in Figure 6 shows that those additional  
14 elements which decrease the scaling rate. These elements could corresponds to organic  
15 molecules, humic substances or suspended matter (clay...), in line with the results of the  
16 literature (Ladel and Leroy, 1997). They may poison the active sites of the CaCO<sub>3</sub> crystals  
17 and thus strongly influence the deposition process. The surface charges of these elements  
18 could play a role in those mechanisms. For example, Hui et al. showed that the antiscaling  
19 effect of clays is maximum if the clay displays the maximum quantity of suspended materials  
20 as well as a highly negative zeta ( $\zeta$ ) potential (Hui et al., 2004).

21           Figure 6B shows a comparison of the mass change of scale deposition for Salvetat  
22 water (curve a) and Salvetat water diluted at 50% (curve b). The supersaturation coefficient is  
23 slightly higher for Salvetat water diluted at 50% than for Salvetat water (9.60 and 8.45  
24 respectively). It must be noticed that the scaling rate is higher for Salvetat water than for  
25 Salvetat water diluted at 50%. Indeed, the Ca<sup>2+</sup> concentration is lower, and the scaling rate

1 decreased when the concentration of calcium decreased, *i.e.* the number of CaCO<sub>3</sub> nuclei  
2 decreased. The supersaturation coefficient is therefore not the only one parameter which  
3 influences the scaling rate.

4

#### 5 **4. Conclusion**

6 In this work, a scaling quartz crystal microbalance (SQCM) with a pre-calcified  
7 surface constituted of pure calcite was used to assess the scaling propensity of synthetic or  
8 natural water.

9 The scaling rate on the pre-calcified surface was markedly dependent on solution  
10 supersaturation coefficient and temperature; it increased with the increase of these two  
11 parameters. For the first time, the activation energy related to a scaling process on an  
12 immobilized CaCO<sub>3</sub> layer (22 kJ.mol<sup>-1</sup>) was evaluated by using SQCM. The kinetics of scale  
13 deposition increased with the flow rate. This phenomenon may be therefore controlled by the  
14 diffusion of ions and/or CaCO<sub>3</sub> nuclei in solution.

15 Finally, the SQCM set-up is sensitive enough to show that scaling rate is lower in  
16 natural water, compared to synthetic water in similar conditions. This may be due to the  
17 presence of the organic compounds or particle suspensions in natural water which could have  
18 some significant inhibition effects.

19 This work confirms that SQCM is a convenient and sensitive tool to measure *in situ*  
20 CaCO<sub>3</sub> nuclei deposit both in synthetic and natural water. Even at the beginning of the  
21 experiment with small CaCO<sub>3</sub> particles at low concentration, it could be used as an *in situ*  
22 sensor to assess the scaling propensity for a given water, immersed in a main circuit or in a  
23 bypass. This could be interesting for some industrial applications (*i.e.* cooling system or  
24 circuit). It could also be used profitably to assess efficiency of an antiscalant treatment by  
25 considering the scaling propensity of water.

1

2 **Acknowledgement**

3 Cyrille Bazin (LISE) is gratefully thanked for technical assistance on X-Ray diffraction  
4 experiment. Axel Desnoyers de Marbaix (LISE) is thanked for the manufacturing of the QCM  
5 cell.

6

7

1 **Figure captions**

2 **Figure 1:** Scheme of a SQCM set up.

3 **Figure 2:** XRD spectrum of the  $\text{CaCO}_3$  layer formed during the pre-calcifying process. C:  
4 calcite.

5 **Figure 3:** Curves of mass change as a function of time for synthetic water with (a) a pre-  
6 calcified surface (pure calcite) (scaling time  $V_s=1.2 \mu\text{g}\cdot\text{cm}^{-2}\cdot\text{min}^{-1}$ ) and (b) a bare gold  
7 surface (initial  $[\text{Ca}^{2+}]=200 \text{ mg/L}$ ,  $T=30^\circ\text{C}$ , flow rate= $2 \text{ mL}\cdot\text{min}^{-1}$ ,  $\delta=40$ ).

8 **Figure 4:** Mass change as a function of time: influence of the supersaturation coefficient  
9 ( $T=30^\circ\text{C}$ , flow rate= $2 \text{ mL}\cdot\text{min}^{-1}$ , pre-calcified surface of the sensor made of pure calcite).

10 **Figure 5:** Logarithm of the scaling rate  $V_s$  as a function of the logarithm of  $\delta$  at (■)  $30^\circ\text{C}$  and  
11 (▲)  $40^\circ\text{C}$  (flow rate= $2 \text{ mL}\cdot\text{min}^{-1}$ , pre-calcified surface of the sensor made of pure calcite).

12 **Figure 6:** (A) Mass change of scale deposited from (a) synthetic water ( $[\text{Ca}^{2+}]=200 \text{ mg}\cdot\text{L}^{-1}$ ,  
13  $\delta=20$ ), (b) Salvetat water ( $\delta = 21$ ). (B) Mass change of scale deposited from (a) Salvetat water  
14 ( $\delta = 8.45$ ) and (b) Salvetat water diluted at 50% ( $\delta = 9.60$ ). Flow rate= $2 \text{ mL}\cdot\text{min}^{-1}$ ,  $30^\circ\text{C}$ , pre-  
15 calcified surface of the sensor made of pure calcite.

16

17

18 **Table captions**

19 **Table 1:** Concentration of ions in Salvetat® water.

20 **Table 2:** Summary of data obtained from fitted curves (see text for signification of the  
21 parameters).

22

23

24

25



## 1 **References**

- 2 Abd-El-Khaled, D. E., Abd-El-Nabey, B. A., 2013. Evaluation of sodium hexametaphosphate  
3 as scale and corrosion inhibitor in cooling water using electrochemical techniques.  
4 *Desalination* 311, 227–233.
- 5 Abdel-Aal, N., Satoh, K., Sawada, K., 2002. Study of the adhesion mechanism of  $\text{CaCO}_3$   
6 using a combined bulk chemistry/QCM technique. *Journal of Crystal Growth* 245, 87–100.
- 7 Al Nasser, W. N., Al Salhi, F. H., 2013. Scaling and aggregation kinetics determination of  
8 calcium carbonate using inline technique. *Chemical Engineering Science* 86, 70–77.
- 9 Ben Amor, M., Zgolli, D., Tlili, M. M., Manzola, A. S., 2004. Influence of water hardness,  
10 substrate nature and temperature on heterogeneous calcium carbonate nucleation.  
11 *Desalination* 166, 79–84.
- 12 Bizet, K., Gabrielli, C., Perrot, H., 2000. Immunodetection by quartz crystal microbalance –  
13 A new approach for direct detection of rabbit IgG and peroxidase. *Applied Biochemistry and*  
14 *Biotechnology* 89, 139–150.
- 15 Blum, A. E., Yund, R.A., Lasaga, A. C., 1990. The effect of dislocation density on the  
16 dissolution rate of quartz. *Geochim. Cosmochim. Acta* 54, 283–297.
- 17 Brecevic, L., Kralj, D., 2007. On calcium carbonates: from fundamental research to  
18 application. *Croat. Chem. Acta* 80, 467–484.
- 19 Cassford, G. E., House, W. A., Pethybridge, A. D., 1983. Crystallisation kinetics of calcite  
20 from calcium bicarbonate solutions between 278.15 and 303.15 K. *J. Chem. Soc. Faraday*  
21 *Trans* 79, 1617–1632.
- 22 Chao, Y., O. Horner, F. Hui, J. Lédion, H. Perrot, 2014a. Direct detection of calcium  
23 carbonate scaling via a pre-calcified sensitive area of a quartz crystal microbalance,  
24 *Desalination* 352, 103–108.

1 Chao, Y., Horner, O., Vallée, P., Meneau, F., Alos-Ramos, O., Hui, F., Turmine, M., Perrot,  
2 H., Lédion, J., 2014b. In situ probing calcium carbonate formation by combining fast  
3 controlled precipitation method and small-angle X-ray scattering. *Langmuir* 30, 3303–3309.

4 Chao, Y., 2016. Scaling Potential determination of water circuit by the use of an ultrasensitive  
5 crystal quartz microbalance. 2013, PhD Thesis, Université Pierre et Marie Curie (France).

6 Chen, T., Neville, A., Yuan, M., 2005. Calcium carbonate scale formation – assessing the  
7 initial stages of precipitation and deposition. *J. Petrol. Sci. Eng.* 46, 185–194.

8 Demichelis, R., Raiteri, P., Gale, J. D., Quigley, D., Gebauer, D., 2011. *Nature*  
9 *Communications* 2, 1-8. Donnet, M., Aimable, A., Lemaître, J., Bowen, P., 2010. Contribution  
10 of aggregation to the growth mechanism of seeded calcium carbonate precipitation in the  
11 presence of polyacrylic acid. *J. Phys. Chem B* 114, 12058–12067.

12 Gabrielli, C., Keddad, M., Maurin, G., Perrot, H., Rosset, R., Zidoune, M., 1996. Estimation  
13 of the deposition rate of thermal calcareous scaling by the electrochemical impedance  
14 technique. *Journal of Electrochemical Chemistry* 412, 189–193.

15 Gabrielli, C., Keddad, M., Khalil, A., Maurin, G., Perrot, H., Rosset, R., Zidoune, M., 1998.  
16 Quartz crystal microbalance investigation of electrochemical calcium carbonate scaling. *J.*  
17 *Electrochem. Soc.* 145, 2386–2396.

18 Gabrielli, C., Maurin, G., Poindessous, G., Rosset, R., 1999. Nucleation and growth of  
19 calcium carbonate by an electrochemical scaling process. *Journal of Crystal Growth* 200,  
20 236–250.

21 Gauthier, G., Chao, Y., Horner, O., Alos-Ramos, O., Hui, F., Lédion, J., Perrot, H., 2012.  
22 Application of the Fast Controlled Precipitation method to assess the scale-forming ability of  
23 raw river waters. *Desalination* 299, 89–95.

24 Hasson, D., Bramson, D., Limoni-Relis, B., Semiat, R., 1996. Influence of the flow system on  
25 the inhibitory action of aCO<sub>3</sub> scale prevention additives. *Desalination* 108, 67–79.



1 Hillig, W. B., 1966. A derivation of classical two-dimensional nucleation kinetics and the  
2 associated crystal growth laws. *Acta Metallurgica* 14, 1868 – 1869.

3 Hui, H., Lédion, J., 2002. Evaluation methods for the scaling power of water. *Eur. J. Water*  
4 *Qual.*, 33, 41 – 52.

5 Hui, F., Yang, Y., Lédion, J., 2003. Evaluation gravimétrique des vitesses d'entartrage sur  
6 tubes témoins. *Journal Européen d'Hydrologie* 34, 221 – 234.

7 Hui, F., Palmier, C., Jan, Y., Orain, Y., Baron, J., Lédion, J., 2004. Influence of clay  
8 suspensions on scaling. *European Journal of Water Quality* 35, 11 – 28.

9 Keysar, S., 1994. Effect of surface roughness on the morphology of calcite crystallizing on  
10 mild steel. *Journal of Colloid and Interface Science* 162, 311 – 319.

11 Kitano, Y., Hood, D. W., 1965. The influence of organic material on the polymorphic  
12 crystallization of calcium carbonate. *Geochimica et Cosmochimica Acta* 29, 29 – 41.

13 Koutsoukos, P. G., Kontoyannis, C. G., 1984. Precipitation of calcium carbonate in aqueous  
14 solutions. *J. Chem. Soc. Faraday trans. 1*, 80, 1181 – 1192.

15 Ladel, J., Leroy, P., 1997. Mise en évidence de l'effet inhibiteur de métabolites d'algues  
16 planctoniques sur la précipitation du carbonate de calcium dans les eaux naturelles d'origine  
17 superficielle. *Journal Européen d'Hydrologie* 28, 69 – 86.

18 Lédion, J., Leroy, P., Labbé, J. P., 1985. Détermination du caractère incrustant d'une eau par  
19 un essai d'entartrage accéléré. *T.S.M. L'eau*, 80<sup>ème</sup> année, 323 – 328.

20 Legrand, L., Poirier, G., Leroy, P., 1981. Les équilibres carboniques et l'équilibre calco-  
21 carbonique dans les eaux naturelles. Eyrolles, Paris.

22 Leroy, P., Lin, W., Lédion, J., Khalil, A., 1993. Caractérisation du pouvoir entartrant des eaux  
23 à l'aide d'essai d'électrodéposition – étude comparative de plusieurs méthodes. *J. Water SRT-*  
24 *Aqua* 42, 23 – 29.

1 Morse, J. W., Arvidson, R. S., Lüttge, A., 2007. A calcium carbonate formation and  
2 dissolution. *Chem. Rev.* 107, 342 – 381.

3 Nancollas, G. H., Reddy, M. M., 1971. The crystallization of calcium carbonate, II. Calcite  
4 growth mechanism. *Journal of Colloid and Interface Science* 37, 824 – 830.

5 Packter, A., 1968. The precipitation of sparingly soluble alkaline-earth metal and lead salts:  
6 nucleation and growth orders during the induction time. *J. Chem. Soc. (A)*, 859 – 862.

7 Parlaktuna, M., Okandan, E., 1989. The use of chemical inhibitors for prevention of calcium  
8 carbonate scaling. *Geothermics* 18, 241 – 248.

9 Parsiegla, K. I., Katz, J. L., 1999. Calcite growth inhibition by copper(II). I. Effect of  
10 supersaturation. *Journal of Crystal Growth* 200, 213 – 226.

11 Peronno, D., Cheap-Charpentier, H., Horner, O., Perrot, H., 2015. Study of the inhibition  
12 effect of two polymers on calcium carbonate formation by fast controlled precipitation  
13 method and quartz crystal microbalance. *Journal of Water Process Engineering* 7, 11–20.

14 Plummer, N. L., Busenberg, E., 1982. The solubilities of calcite, aragonite and vaterite in  
15 CO<sub>2</sub>-H<sub>2</sub>O solutions between 0 and 90°C, and an evaluation of the aqueous model for the  
16 system CaCO<sub>3</sub>-CO<sub>2</sub>-H<sub>2</sub>O. *Geochimica et Cosmochimica Acta* 46, 1011 – 1040.

17 Sauerbrey, G., 1959. Verwendung von Schwingquarzen zur Wägung dünner Schichten und  
18 zur Mikrowägung. *Zeitschrift für Physik* 155, 206 – 222.

19 Tlili, M. M., Benamor, M., Gabrielli, C., Perrot, H., Tribollet, B., 2003. Influence of the  
20 interfacial pH on electrochemical CaCO<sub>3</sub> precipitation. *Journal of the Electrochemical Society*  
21 150, C765 – C771.

22 Xyla, A. G., Giannimaras, E. K., Koutsoukos, P. G., 1991. The precipitation of calcium  
23 carbonate in aqueous solutions. *Colloids and Surfaces* 53, 241 – 255.

24 Yang, Q., 2002. Investigation of induction period and morphology of CaCO<sub>3</sub> fouling on  
25 heated surface. *Chemical Engineering Science* 57, 921 – 931.

- 1 Zhang, Y., Shaw, H., Farquhar, R., Dawe, R., 2001. The kinetics of carbonate scaling –
- 2 application for the prediction of downhole carbonate scaling. *J. Petrol. Sci. Eng.* 29, 85 – 95.